1-1-2013

Numerical solution of stone column improved soft soil considering arching, clogging and smear effects

Buddhima Indraratna
University of Wollongong, indra@uow.edu.au

Sudip Basack
Bengal Engineering and Science University

Cholachat Rujikiatkamjorn
University of Wollongong, cholacha@uow.edu.au

Numerical solution of stone column improved soft soil considering arching, clogging and smear effects

Abstract

Improvement of soft clay deposits by the installation of stone columns is one of the most popular techniques followed worldwide. The stone columns not only act as reinforcingmaterial increasing the overall strength and stiffness of the compressible soft soil, but they also promote consolidation through effective drainage. The analytical and numerical solutions available for ascertaining the response of column-reinforced soil have been developed on the basis of the equal strain hypothesis. For typical surcharge (embankment) loading, the free strain analysis appears to give more realistic results comparable to field data. The paper presents a novel numericalmodel (finite-differencemethod) to analyze the response of stone column-reinforced soft soil under embankment loading, adopting the free strain approach and considering both arching and clogging effects. Apart from predicting the dissipation of excess pore water pressure and the resulting consolidation settlement with time, the load transfer mechanismand the extent of ground improvement are some of the salient features captured by the proposedmodel. The proposedmodel is validated by comparing with existingmodels and field data, which indicate the suitability and accuracy of the solutions. The proposed model is also applied successfully to selected case studies.

Keywords

soil, column, effects, soft, arching, considering, improved, solution, stone, clogging, smear, numerical

Disciplines

Engineering | Science and Technology Studies

Publication Details

Indraratna, B., Basack, S. & Rujikiatkamjorn, C. (2013). Numerical solution of stone column improved soft soil considering arching, clogging and smear effects. Journal of Geotechnical and Geoenvironmental Engineering, 139 (3), 377-394.

Numerical Solution of Stone Column–Improved Soft Soil Considering Arching, Clogging, and Smear Effects

Buddhima Indraratna, F.ASCE[1]; Sudip Basack[2]; and Cholachat Rujikiatkamjorn[3]

Abstract: Improvement of soft clay deposits by the installation of stone columns is one of the most popular techniques followed worldwide. The stone columns not only act as reinforcing material increasing the overall strength and stiffness of the compressible soft soil, but they also promote consolidation through effective drainage. The analytical and numerical solutions available for ascertaining the response of column-reinforced soil have been developed on the basis of the equal strain hypothesis. For typical surcharge (embankment) loading, the free strain analysis appears to give more realistic results comparable to field data. The paper presents a novel numerical model (finite-difference method) to analyze the response of stone column–reinforced soft soil under embankment loading, adopting the free strain approach and considering both arching and clogging effects. Apart from predicting the dissipation of excess pore water pressure and the resulting consolidation settlement with time, the load transfer mechanism and the extent of ground improvement are some of the salient features captured by the proposed model. The proposed model is validated by comparing with existing models and field data, which indicate the suitability and accuracy of the solutions. The proposed model is also applied successfully to selected case studies. **DOI: 10.1061/(ASCE)GT.1943-5606.0000789.** © *2013 American Society of Civil Engineers.*

CE Database subject headings: Finite difference method; Foundation settlement; Numerical models; Soft soils; Soil permeability; Stone columns; Arches.

Author keywords: Finite-difference method; Foundation settlement; Numerical models; Soft soils; Soil permeability; Stone columns.

Introduction

Reducing long-term settlement of infrastructure and providing cost-effective foundations with sufficient load-bearing capacities are national priorities for infrastructure development in most countries. Soft soil foundations can cause excessive settlement, initiating undrained failure of the infrastructure if proper ground improvement is not carried out (Indraratna et al. 1992). Therefore, it is imperative to apply adequate ground improvement techniques to the existing soft soils before construction to prevent unacceptable excessive and differential settlement and increase the bearing capacity of the foundations.

Among various methods of soft soil improvement, reinforcing the ground by installing stone columns is one of the well-established and effective techniques practiced worldwide (Wang 2009). As reported by Guetif et al. (2007), the stone columns not only act as reinforcement, possessing greater strength and stiffness in comparison with the surrounding soil, but they also speed up the time-dependent dissipation of excess pore water pressure caused by surcharge loading due to shortening the drainage path.

Various analytical and numerical solutions have already been developed for understanding the load transfer mechanism of soft soil reinforced with stone columns. Among the most significant contributions, the studies by Alamgir et al. (1996), Wang (2009), Han and Ye (2000, 2002), Malarvizhi and Ilamparuthi (2008), Lo et al. (2010), and Murugesan and Rajagopal (2010) are noteworthy. All of these solutions are based on the unit cell analysis assuming the equal strain hypothesis. Alamgir et al. (1996) carried out a free strain analysis, but the time-dependent consolidation of soil was not considered. However, the equal strain assumption is strictly valid only when the surcharge load applied on the ground surface is of a rigid nature. Understandably, this will result in an unequal distribution of stress induced on the soil surface. In the case of embankment loading, the flexible nature of the applied surcharge is most likely to induce an equal distribution of surface load resulting in uneven surface settlement or free strain, as described by Barron (1948). However, the true nature of embankment surcharge loading is neither fully flexible nor purely rigid, but at an intermediate state between the free strain and equal strain conditions. Terzaghi (1943) showed that the flexibility of the granular platform depends on both its density and thickness. In the field, it is suggested that the overall shear stiffness of the platform is to be measured for classifying the loading distribution pattern. The equal strain condition occurs when the platform layer thickness and the soil density increase.

In the field, in the proximity of the embankment centerline, the condition of negligible lateral displacement can be justified by the use of the unit cell approach. In the past, Lorenzo and Bergado (2003) and Murugesan and Rajagopal (2010) successfully demonstrated the use of unit cell analysis to capture the behavior of soil

[1]Professor, School of Civil, Mining and Environmental Engineering, Faculty of Engineering, Univ. of Wollongong, Wollongong City, NSW 2522, Australia; and Director, Centre for Geomechanics and Railway Engineering, Faculty of Engineering, Univ. of Wollongong, Wollongong City, NSW 2522, Australia; and Program Leader, Australian Research Council Centre of Excellence in Geotechnical Science and Engineering, The University of Newcastle, Callaghan, NSW 2308, Australia (corresponding author). E-mail: indra@uow.edu.au

[2]Associate Professor, Bengal Engineering and Science Univ., Howrah, West Bengal 711103, India; formerly, Endeavour Postdoctoral Research Fellow of Australian Government, Centre for Geomechanics and Railway Engineering, Univ. of Wollongong, Wollongong City, NSW 2522, Australia.

[3]Senior Lecturer, Centre for Geomechanics and Railway Engineering, Univ. of Wollongong, Wollongong City, NSW 2522, Australia; and Australian Research Council Centre of Excellence in Geotechnical Science and Engineering, The University of Newcastle, Callaghan, NSW 2308, Australia.

Note. This manuscript was submitted on October 21, 2010; approved on June 13, 2012; published online on August 1, 2012. Discussion period open until August 1, 2013; separate discussions must be submitted for individual papers. This paper is part of the ***Journal of Geotechnical and Geoenvironmental Engineering***, Vol. 139, No. 3, March 1, 2013. ©ASCE, ISSN 1090-0241/2013/3-377–394/$25.00.

improved by stone columns at the centerline of the embankment. However, the authors agree that the unit cell analysis may not successfully predict the overall behavior in a large project where hundreds of columns are installed, and it is recognized that the analysis would only be accurate at the proximity to the embankment centerline. Elsewhere, i.e., toward the embankment toe, the single column analysis deviates from accuracy because of the nonuniform surcharge load distribution, large strain conditions, increased lateral yield, effects of changing embankment geometry, and heave at the toe.

For a typical fill embankment, the behavior of the soil-stone column system is time dependent. Initially, most of the imposed total stress is taken by the increased (excess) pore water pressure. Because of the dissipation of excess pore pressure, progressive settlement of the soft clay and arching occurs, where the weight of the fill is expected to arch over to the stone columns, resulting in an uneven distribution of vertical stress on the ground surface. This phenomenon is duly supported by numerous other studies (Low et al. 1994; Abusharar et al. 2009; Deb 2010).

Because of the migration of clay particles from soil into the pores of the column, a clogged zone may be formed within the column in the vicinity of the soil-column interface (Adalier and Elgamal 2004). Also, as a result of installation, a smear zone is developed in the soil adjacent to this interface (Han and Ye 2002).

Numerical Analysis

The numerical model is formulated considering a steady and uniform load intensity imposed on the ground surface caused by the self-weight of the embankment, apart from the instantaneous surcharge load applied at the top of the embankment. The average load intensity on the ground surface may therefore be written as

$$\overline{q} = q_s + \gamma_e H_e \tag{1}$$

where q_s = uniform surcharge load intensity on the embankment fill, and γ_e and H_e = unit weight and maximum height of the embankment, respectively.

Statement of the Problem

The idealized problem is depicted in Figs. 1(a and b). The soft clay layer of thickness H has been assumed to overlay on an impervious rigid boundary and is improved by a group of stone columns having a radius of r_c each, extended to the bottom of the clay layer. The unit cell approach that adequately represents the true response of reinforced ground (Balaam et al. 1977) is considered in the current analysis. As described by Wang (2009), the radius of the influence of the unit cell is calculated by

$$r_e = s_g s \tag{2}$$

where s = center-to-center distance between the adjacent columns, and s_g = geometric constant that depends on the pattern of stone column installation.

The cross section of the entire zone of the unit cell is divided into four distinct zones [Fig. 1(c)], viz., the unclogged column zone, the clogged column zone, the smear zone adjacent to the column, and the outer undisturbed soil zone. As shown in Fig. 2, the soil mass within the unit cell was divided both radially and vertically into $(m-1)$ and $(n-1)$ number of equal divisions, respectively; m and n are positive integers greater than unity, such that each of these divisions may be expressed, respectively, as $\delta r = (re - rc)/(m-1)$ and $\delta z = H/(n-1)$. The total time interval of computation t_t is divided into $(p-1)$ number of equal divisions, i.e., $\delta t = t_t/(p-1)$. The primary objective of the analysis is to compute the excess pore water pressures and the effective stresses developed at each separator at the corresponding time and thereby compute the other time-dependent variables such as the degree of consolidation. In this paper, these separators are denoted as nodes. The soil elements are understandably ring-shaped.

The specific time t_t is the desired time of computation to be chosen arbitrarily, and it is not the total time required to achieve the desired degree of consolidation. The parameters for soil consolidation and settlement are computed at the end of this time interval t_t. If necessary, further computation can be carried out using these values as the initial input parameters and choosing a new time interval t_t.

Han and Ye (2002) stated that for a typical stone column, r_s/r_c varies from 1 to 1.2 and k_h/k_s is usually in the order of 10, where, r_s is the radius of smear zone, and k_h and k_s are the horizontal permeability of soil in the undisturbed and smear zones, respectively. In the analysis of Wang (2009), the value of r_s/r_c was assumed in the range of 1–2 and k_s/k_h as 0.1. As reported by Walker and Indraratna (2006), the ratio of r_s/r_c usually varies between 2 and 3, and the permeability of soil in the smear zone decreases in a parabolic pattern with radial distance.

The phenomenon of clogging is separately discussed in the section, Effect of Clogging.

Assumptions

The analysis was carried out based on the following assumptions:

1. All the compressive strains within the soil mass and the stone column occur only in the vertical direction;
2. The elastic settlements of the ground and the column are insignificant compared with the consolidation settlement;
3. The soil is fully saturated and the water is incompressible;
4. Darcy's law is valid, and the flow of water through the soil is purely horizontal (radial toward the column). No flow of water takes place through the cylindrical boundary and the impervious base of the unit cell; and
5. The coefficients of permeability and compressibility of the soil remain constant during the process of consolidation.

Arching Effect

Soil arching is a common phenomenon for stone column–reinforced soft soil beneath embankments. Arching initiates a reduction of the vertical stress acting on the relatively soft soil while increasing in the vertical stress on the stiffer columns (Deb 2010). As pointed out by Low et al. (1994), the arching effect induces a nonuniform distribution of vertical stress on the ground surface [Fig. 3(a)].

Load Transfer at the Interface between Soil and Column

As discussed by Han and Ye (2002), one of the major differences between stone columns and drain wells is that stone columns have a higher stiffness ratio of the columns to the soil, resulting in a much greater stress transfer from the soil to the columns. Immediately after the embankment load is applied on the reinforced ground surface, both the column and the surrounding soil undergo undrained elastic settlements. With the assumptions that the deformations take place only along the vertical direction and there is no differential settlement at the interface between the column and the surrounding soil, the ratio of vertical stresses induced at the interface between the column and the soil has been found proportional to the modular ratio of the reinforced soft ground (Han and Ye 2000; Castro and Sagaseta 2009). Denoting the ratio of the stress on the stone column to that on the surrounding soil as n_s, the steady stress concentration ratio, the following equation was obtained:

J. Geotech. Geoenviron. Eng. 2013.139:377-394.

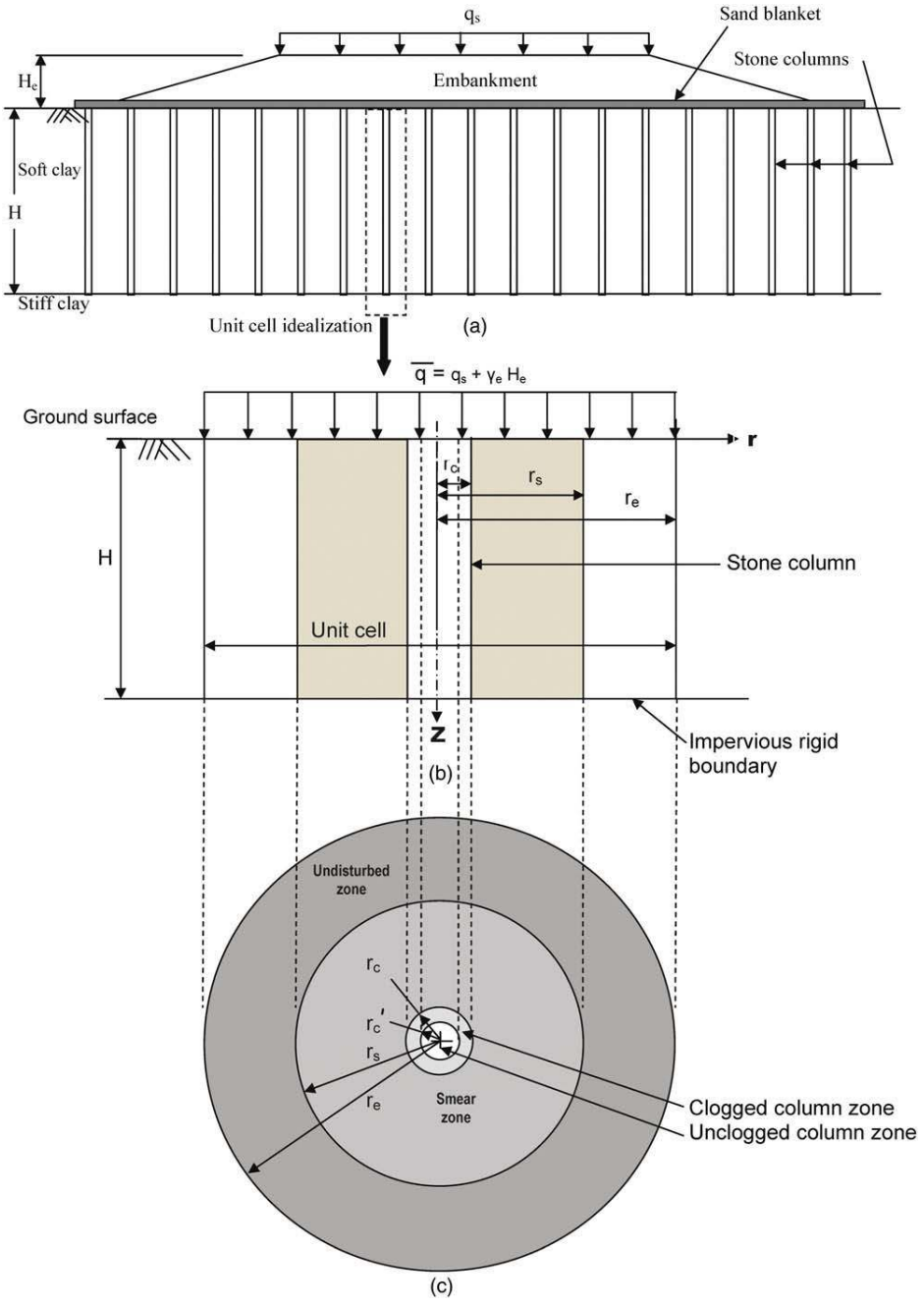

Fig. 1. (a) Typical stone column–reinforced soft clay deposit supporting an embankment; (b) unit cell idealization; (c) cross section of the unit cell

$$q_c/q_1 = n_s \tag{3a}$$

where q_c and q_1 = average vertical stresses on the column and the soil at the ground surface, respectively, at the interface, and n_s = steady stress concentration ratio.

With the progressive bulging of the column in the vicinity of the ground surface and the development of plastic strain, the stress concentration ratio changes with time. In this analysis, however, the bulging of column was not considered; thus, the computed settlements remain constant at the interface. Following the analysis of Han and Ye (2000) regarding the coefficient of compressibility of an elastic body, the following correlation between n_s and the elastic moduli of the column and the soil was introduced:

$$n_s = \chi \frac{E_c}{E_s} \tag{3b}$$

where E_c and E_s = elastic moduli of the column and the surrounding soil, respectively, and χ = function of the Poisson's ratios of the soil and the column.

As mentioned by Castro and Sagaseta (2009), the constrained modular ratio between the column and soil varies in the range of 10–50, although the lateral expansion of the column (bulging) reduces the stress concentration ratio n_s significantly. They also mentioned that the plastic strains developed in the column can further reduce the value of n_s to a value as low as 5. On the basis of the theoretical and experimental investigations conducted by Barksdale and Bachus

J. Geotech. Geoenviron. Eng. 2013.139:377-394.

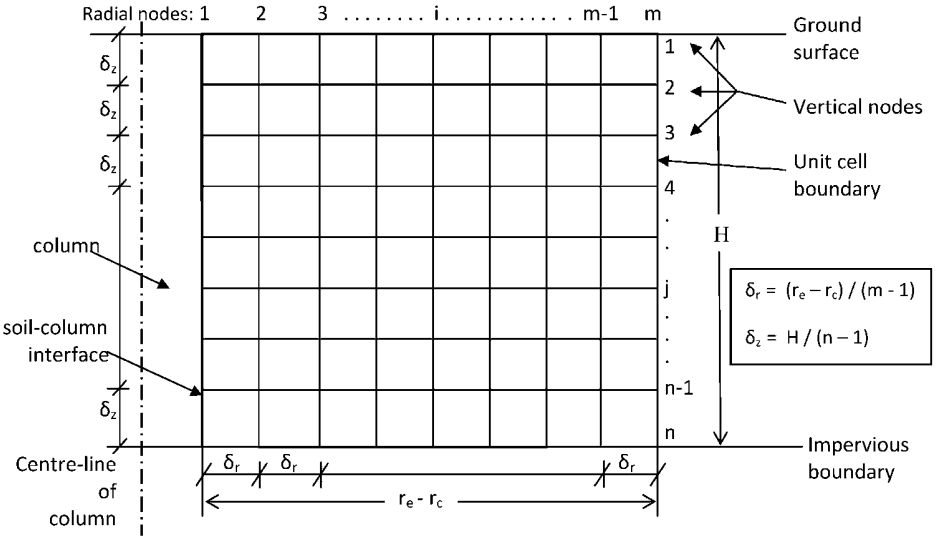

Fig. 2. Discretization of soil into elements within the unit cell

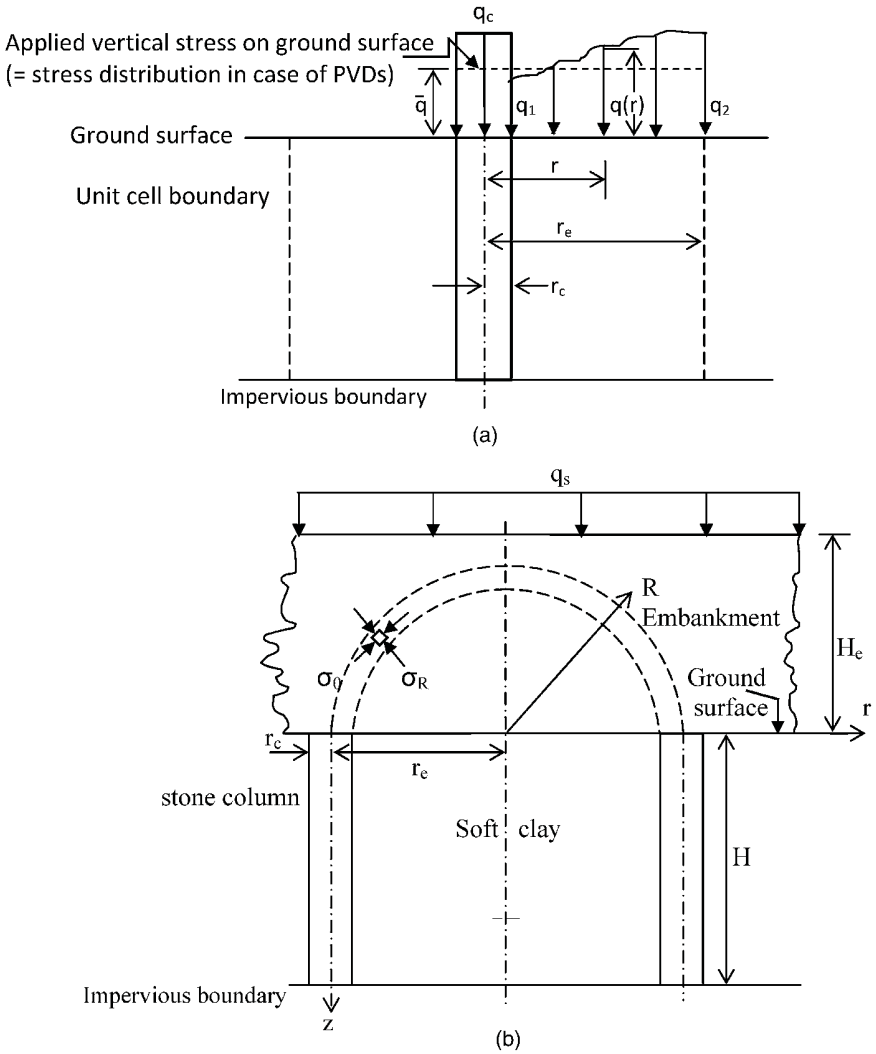

Fig. 3. (a) Vertical stress distribution on the ground surface; (b) arching effect in the embankment

J. Geotech. Geoenviron. Eng. 2013.139:377-394.

(1983), the range of n_s was reported as 3–10, whereas Mitchell (1981) reported this range to be 2–6 based on field studies. As further suggested by Han and Ye (2002), the typical value of n_s ranges between 2–5.

Vertical Stress Distribution on Soil

Following the analysis of Low et al. (1994), the compatibility equation for the element within the embankment material shown in Fig. 3(b) can be written as

$$\frac{d\sigma_R}{dR} + \frac{\sigma_R - \sigma_\theta}{R} + \gamma_e = 0 \tag{4}$$

where σ_R and σ_θ = stresses in the soil element along the directions of the global coordinates R and θ, respectively.

For limit analysis, $\sigma_\theta = K_p\sigma_R$, where K_p is the coefficient of passive earth pressure of the embankment material. Therefore, Eq. (4) can be written as

$$\frac{d\sigma_R}{dR} + \frac{\sigma_R(1 - K_p)}{R} + \gamma_e = 0 \tag{5}$$

Considering the value of radial stress σ_R along the midway between the consecutive columns at $R = r_e$ as the boundary condition, i.e., $\sigma_R = \gamma_e(H_e - r_e) + q_s$ at $R = r_e$, the solution to the differential equation [Eq. (5)] can be expressed by

$$\sigma_R = \left[\gamma_e(H_e - r_e) + q_s - \gamma_e r_e/(2K_p - 2)\right] \times (R/r_e)^{(2K_p - 1)} + \gamma_e R/(2K_p - 2) \tag{6}$$

Following the analysis of Abusharar et al. (2009), the imposed load intensity on the ground surface at $r = r_e$ may be written as

$$q_2 = \gamma_e r_c(N - 1)(K_p - 1)/(K_p - 2) + \left[q_s + \gamma_e H_e - (K_p - 1)/(K_p - 2)\right](1 - 1/N)^{(K_p - 1)} \tag{7}$$

where $N = r_e/r_c$.

The stone columns possess higher stiffness in comparison with the surrounding softer soil. Because of this significant column to soil stiffness ratio and the flexible nature of the embankment, the fill weight would arch over the stone columns (Lo et al. 2010) and impose an uneven load distribution on the surface [as represented by Eq. (8*d*)]. When the external load is applied on the unit cell, the column deforms under the loading, and the surrounding soil offers passive resistance against the outward lateral strains of the column.

Therefore, the passive state is enforced only at the soil column interface and not anywhere else in the soft soil within the unit cell where the K_0 state is valid. During the process of consolidation, the soil in the unit cell remains at the K_0 state, although differential settlement occurs at the soil surface following the free strain hypothesis (described in the subsection Consolidation of Soft Clay) that results in the development of vertical shear stress. Considering a passive state to occur in the fill in the region above the stone column (Fig. 3), the value of q_2 is justified.

The imposed load intensity on the soil surface at a radial distance r is hereby denoted as $q(r)$, which was quantified using the following boundary conditions:

1. The imposed load intensity on the ground surface over the boundary of the unit cell is q_2, i.e.,

$$q(r_e) = q_2 \tag{8a}$$

2. Because of the axi-symmetry of the unit cell, the value of $[\partial q(r)]/(\partial r)$diminishes at the boundary of the unit cell; hence

$$\frac{dq(r_e)}{dr} = 0 \tag{8b}$$

3. The total vertical load imposed on the surface of the unit cell is equal to the sum of the loads imposed on the soil and that carried by the column; thus

$$2\pi \int_{r_c}^{r_e} rq(r)dr + q_c\pi r_c^2 = (q_s + \gamma_e H_e)\pi r_e^2 \tag{8c}$$

These conditions are fulfilled when the load distribution function is expressed in the following form:

$$q(r) = q_2 + (N - r/r_c)^2 \frac{(q_s + \gamma_e H_e)N^2 - q_2(N^2 + n_s - 1)}{(N + 3)(N - 1)^3/6 + n_s(N - 1)^2} \tag{8d}$$

The average vertical stress on the soil surface of the unit cell is given by

$$q_{av} = \frac{\overline{q}\pi r_e^2 - q_c\pi r_c^2}{\pi(r_e^2 - r_c^2)} = \frac{\overline{q}N^2 - q_c}{N^2 - 1} \tag{8e}$$

Consolidation of Soft Clay

Dissipation of Excess Pore Pressure

Considering a ring element of soil mass at a radial distance r, depth z, and time t (Fig. 4), the volumetric strain ε_v induced in the soil element is given by (detailed derivation is presented in the Appendix)

$$\frac{\partial\varepsilon_v}{\partial t} = \frac{1}{V}\frac{dV}{dt} = -(k_h/\gamma_w)\left(\frac{1}{r}\frac{\partial u}{\partial r} + \frac{\partial^2 u}{\partial r^2}\right) \tag{9}$$

where ε_v = volumetric strain in the element; V = volume of the element; u = excess pore water pressure; and m_v = coefficient of volume compressibility of the soil. It may be noted that as per Assumption 3, u is a function of the radial distance r and the time t, but not of the depth z. The excess pore pressure at any ith radial node and kth time instant is hereby denoted as $u(i, k)$.

On the basis of Assumption 1, the rate of excess pore pressure dissipation $(\partial u)/(\partial t)$ can then be expressed as

$$\frac{\partial u}{\partial t} = c_{vr}\left(\frac{1}{r}\frac{\partial u}{\partial r} + \frac{\partial^2 u}{\partial r^2}\right) \tag{10}$$

where c_{vr} = coefficient of radial consolidation of the soil = $k_h/(m_v\gamma_w)$.

Expressing Eq. (10) in a finite-difference form, the following matrix equation can be obtained:

$$[A]\{u\} = \{b\} \tag{11}$$

where $[A]$ = coefficient matrix of order $mp \times mp$, $\{u\}$= unknown vector of order $mp \times 1$ for excess pore water pressure, and $\{b\}$= augment vector of order $mp \times 1$.

J. Geotech. Geoenviron. Eng. 2013.139:377-394.

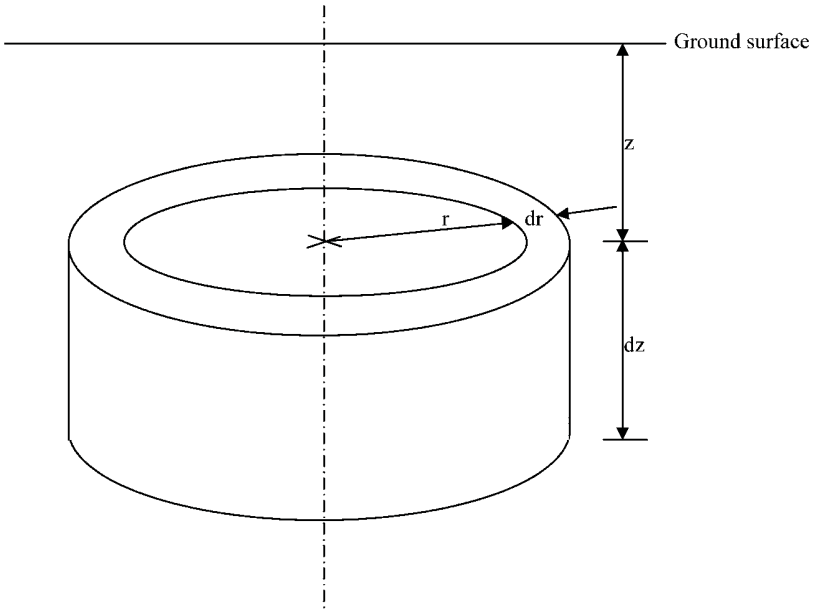

Fig. 4. Typical soil element in the unit cell

The matrices in Eq. (11) are defined in the Appendix.

In formulating $[A]$ in Eq. (11), the following boundary conditions were considered:

1. At $t = 0$, $u(i,k) = u_0(i)$ for $i = 1,2,3,\ldots,m$;
2. Because the column material is assumed as freely draining, no excess pore water pressure is developed at the interface at $t > 0$. Mathematically, $u(1,k) = 0$ for $k = 2,3,4,\ldots,m$; and
3. At $r = r_e$, $\partial u/\partial r = 0$.

Solving Eq. (11), the unknown vector $\{u\}$ can be evaluated.

The average excess pore water pressure $(\overline{u}_t)$ in the soil elements can be expressed by

$$\overline{u}_t = \frac{1}{\pi(r_e^2 - r_c^2)} \int_{r_c}^{r_e} 2\pi r u \, dr = \frac{2}{r_e^2 - r_c^2}\left\{ r_c u(1,k) + r_e u(n,k) + \sum_{i=2}^{m-1} [r_c + (i-1)\delta_r] u(i,k) \right\} \tag{12}$$

The average excess pore water pressure at any given time t is computed as the weighted average of the nodal pore pressures u_{ik} within the soil of the unit cell. The average degree of consolidation is now given by

$$\overline{U}_t = \left(1 - \overline{u}_t/u_0\right) \times 100\% \tag{13}$$

Settlement of Soft Clay

The displacement of a point (r,z) within the soil mass of the unit cell at time t is given by (more details in the Appendix)

$$\rho = -\int_0^t \int_z^H m_v \frac{\partial u(r,z)}{\partial t} dz \, dt \tag{14}$$

Expressed in numerical notation, Eq. (14) can be rewritten as

$$\rho(i,j,k) = m_{vi}[H - (j-1)\delta_z][u(i,1) - u(i,k)] \tag{15a}$$

where m_{vi} is the coefficient of volume compressibility of soil at the ith nodal point.

The average settlement at the ground surface was computed as the weighted average and is expressed by

$$\overline{\rho}(k) = \frac{1}{\pi(r_e^2 - r_c^2)} \int_{r_c}^{r_e} 2\pi r \rho \, dr = \frac{2}{r_e^2 - r_c^2}\left\{ r_c \rho(1,1,k) + r_e \rho(n,1,k) + \sum_{i=2}^{m-1} [r_c + (i-1)\delta_r] \rho(i,1,k) \right\} \tag{15b}$$

Both the permeability and compressibility parameters change non-uniformly with the radial distance within and just outside the smear zone, as elaborated by Indraratna and Redana (1997, 1998), supported by large-scale consolidation test data. However, to simplify the mathematical formulation of already complex equations, a reduced lateral permeability was assumed as an equivalent average (constant) across the smear zone annulus, and accordingly, the lateral coefficient of consolidation (c_{vr}) is also changed proportionately. With this consideration, the coefficient matrix $[A]$ in Eq. (11) was formulated. This assumption may lead to a slight overestimation of the settlement, but it facilitated a useful solution to otherwise complex equations.

Effective Stress in the Soil

The effective stress developed in the soil mass at any point (r,z,t) in the space-time coordinate may be expressed by (Khan et al. 2010)

$$\sigma'(r,z,t) = \gamma' z + q(r) - u(r,t) \tag{16a}$$

where γ' is the effective unit weight of the soil mass.

J. Geotech. Geoenviron. Eng. 2013.139:377-394.

Expressing in numerical notation leads to

$$\sigma'(i,j,k) = \gamma'(j-1)\delta_z + q(i) - u(i,k) \quad (16b)$$

Effect of Clogging

The performance of stone columns in dissipating excess pore pressure can be adversely affected by clogging. Because of the high hydraulic gradient at the soil-column interface, migration of clay particles into the pores of the granular column inevitably occurs, resulting in a significant decrease in the column permeability (Adalier and Elgamalal 2004). This initiates a reduction in the effective radius of the column in terms of drainage, as well as reducing the permeability in the clogged zone. The effective radius of the column with clogging may be expressed by

$$r_c' = \alpha r_c \quad (17)$$

where α = nondimensional factor in the range $0 < \alpha \leq 1$: fresh or ideal stone columns with no clogging are characterized by $\alpha = 1$, whereas total clogging is represented by $\alpha = 0$.

Also, the coefficient of horizontal permeability in the clogged zone may be written as

$$k_{cl} = \alpha_k k_s \quad (18)$$

where α_k = ratio of horizontal permeability of the clogged column zone to that of the smear zone. Limited information (Mays 2010) available about the range of this parameter suggests that $0 < \alpha_k \leq 1$.

Along the radial direction, the entire region including the soil and the clogged zone is discretized into $(m-1)$ number of elements such that $\delta_r = (r_e - r_c')/(m-1)$. In terms of drainage, the permeability of the clogged zone is taken into consideration, and Boundary Condition 2 in section Consolidation of Soft Clay is altered accordingly. The remaining analysis is similar to the case without clogging. The effect of clogging has been studied in terms of the nondimensional parameters α and α_k, the values of which may be reasonably estimated by conducting rigorous experiments (Reddi et al. 2000; Hajra et al. 2002).

Improvement of Soft Clay

During consolidation, the undrained strength and stiffness of the soil increase progressively. Umezaki et al. (1993) developed an analytical model to predict such an increase in undrained shear strength of soft clay as a function of the degree of consolidation. Following this analysis of the correspondence between the effective stress, void ratio, and undrained shear strength of soft clay, the undrained cohesion at any point (i,j,k) in the space-time coordinate system may be written as

$$c_u(i,j,k) = \frac{c_{u0} + \zeta_c(j-1)\delta_z}{1 - \dfrac{e_0 - e(i,j,k)}{m_{vi}(1+e_0)\sigma'(i,j,k)}} \quad (19)$$

where c_{u0} = initial undrained cohesion of the soil at the ground surface; ζ_c = rate of increase of undrained cohesion with respect to depth, assuming the same to be linearly increasing; e_0 = initial void ratio of the soil; $e(i,j,k)$ = reduced void ratio of the soil at point (i,j,k), which may be reasonably estimated from the e-σ' curve. The basis of derivation of Eq. (19) is given in the Appendix.

The undrained shear strength of clay is an important parameter for stability analysis of the embankment. The ground improvement factor ω of the reinforced soil at any kth time instant has been defined as the minimum value of the ratio of the instantaneous to the initial values of the undrained cohesion in the soft soil within the unit cell. Thus

$$\omega = \min[c_u(i,j,k)/c_{u0}] \quad (20)$$

Similarly, the increase in stiffness of the soft soil may be expressed as a settlement factor ξ that is defined herein as the ratio of the average ground settlements of the reinforced to unreinforced soils at 90% consolidation. Similarly, the increase in stiffness of the soft soil caused by reinforcement was expressed as a settlement factor ξ defined as

$$\xi = \frac{\overline{\rho}_{90}}{\overline{\rho}_{u90}} \quad (21)$$

where $\overline{\rho}_{90}$ and $\overline{\rho}_{u90}$ = average settlements at the ground surface of the reinforced and the unreinforced soil at 90% consolidation, respectively. The settlement of unreinforced soil has been computed using Terzaghi's one-dimensional consolidation theory. The settlement values at 90% consolidation are considered practical from a design aspect. Theoretically, the degree of consolidation increases exponentially with time, and it is difficult to compute the final settlement of the reinforced soil at the ground surface at 100% consolidation using the present numerical model.

Computational Algorithm

To execute the analysis, a computer program was written in FORTRAN 90, using the following computational algorithms:

1. Using the input data for soil and column properties, clogging parameters, stress distribution coefficients, embankment characteristics, and time, the vertical stress distributions on the soil surface and the column were calculated by Eq. (8*d*).
2. The nodal excess pore water pressures in the soil were computed using Eq. (11).
3. The average degree of consolidation, nodal and average ground settlements, and nodal effective stresses in the soil are calculated using Eqs. (12)–(16).
4. The improvement and settlement factors are computed.

Validation of the Model

To verify the accuracy of the model developed, some comparisons are made with the available models and field test results. First, the comparison of the average degree of consolidation by radial drainage was only made with the existing models of Han and Ye (2000, 2002) and Wang (2009). The computational parameters adopted are the same as those used by Han and Ye (2002), i.e., $N = 2$, $k_h/k_s = 10$, $r_s/r_c = 1.1$, $H/r_c = 20$, $n_s = 3$, and $\alpha = \alpha_k = 1$. The variations of the average degree of consolidation with the time factor are presented in Fig. 5. The results obtained using the present model are in agreement with the other solutions acceptably close to that of Han and Ye (2002).

Oh et al. (2007) carried out field tests in soft estuarine clays in Queensland, Australia, with a trial embankment incorporating three separate sections: two sections with stone columns of 2- and 3-m spacing (square pattern) and a reference section without any stone columns. A comparison of computed ground settlements using the present methodology with the field results is presented in Fig. 6. The computational parameters used here are adopted from Oh et al.

J. Geotech. Geoenviron. Eng. 2013.139:377-394.

(2007) and are presented in Table 1. The computed settlements, although slightly overpredicted, are in reasonable agreement with the field data. When the clogging effect is incorporated ($\alpha = 0.5$, $\alpha_k = 1$), the predicted settlements are observed to attain values even closer to the field measurements.

Parametric Studies

The numerical model developed was used for understanding the response of a prototype stone column–reinforced soil under step loading. The same field data of Oh et al. (2007) as described in the section Validation of the Model is used for the parametric study, except for the column parameters, which are $r_c = 0.5$ m and $r_e = 1.5$ m. The clogging effect is considered in the analysis. Analysis is carried out with the number of separators $m = n = 31$ with 900 $[=(n-1)^2]$ soil elements and 961$(=n^2)$ nodes.

The time variation of the average degree of consolidation with and without clogging is shown in Fig. 7(a). For a given value of T_r, the degree of consolidation decreases with increasing values of α. Furthermore, for a given value of α, the degree of consolidation decreases with the reduction of α_k. These observations reasonably justify the effect of clogging within the stone column, reflecting the resistance to drainage and thereby retarding the overall consolidation.

The time variation of average excess pore water pressure in the soil with and without clogging is depicted in Fig. 7(b). The average

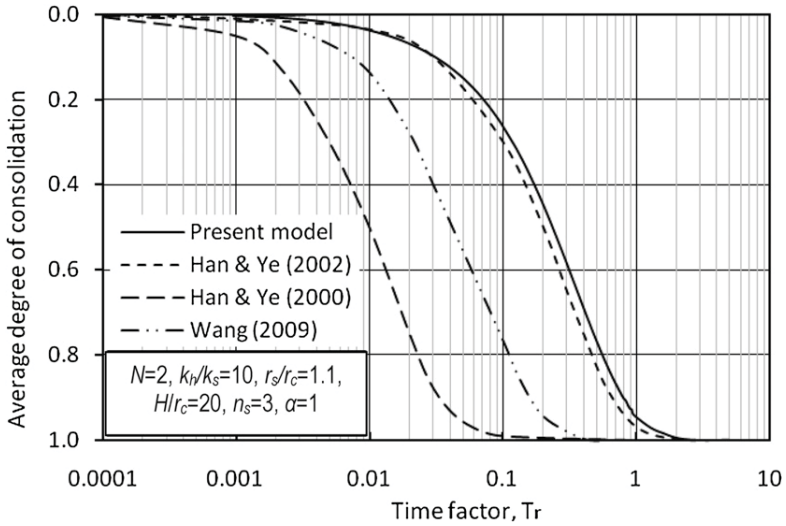

Fig. 5. Comparison of computed rates of consolidation using different methods

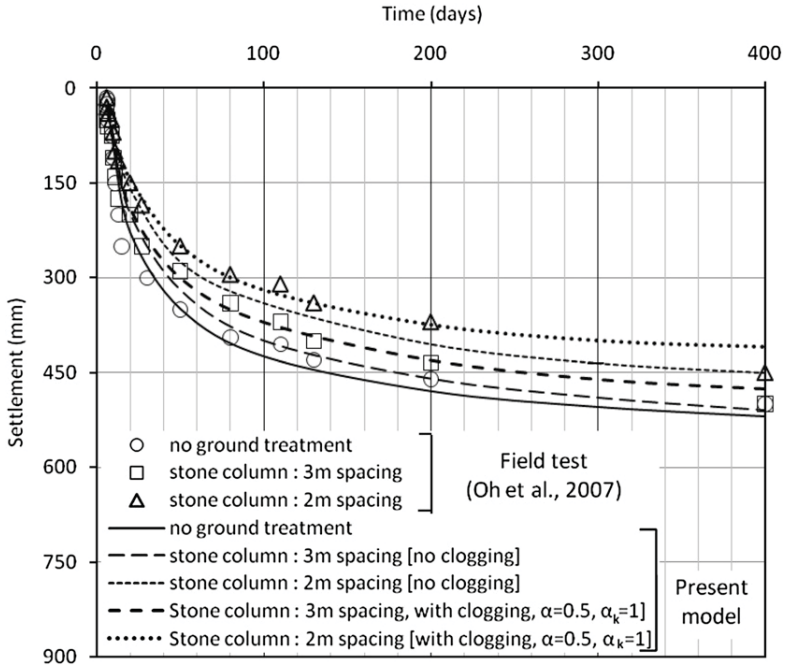

Fig. 6. Comparison of computed settlement with field test results of Oh et al. (2007)

J. Geotech. Geoenviron. Eng. 2013.139:377-394.

Table 1. Input Parameters for the Case Studies

Material	Parameter	Value	
		Oh et al. (2007)	Indraratna (2009)
Soft clay	Coefficient of horizontal permeability (k_h)	1.6×10^{-9}m/s	1×10^{-9}m/s
	Coefficient of volume compressibility (m_v)	2×10^{-6}m^2/N	3×10^{-6}m^2/N
	Normalized horizontal permeability of smear zone (k_s/k_h)	0.1[a]	0.333[b]
	Normalized radius of smear zone (r_s/r_c)	1.15[a]	2.5[b]
	Depth of soft clay (H)	16 m	20 m
Embankment	Height (H_e)	4 m	4.3 m
	Unit weight (γ_e)	20 kN/m^3	20 kN/m^3
	Imposed load intensity on the embankment (q_s)	0	0
	Passive earth pressure coefficient (K_p)	3[c]	3[c]
Stone column/PVD	Radius of stone column/PVD (r_c)	0.5 m	0.017 m
	Radius of unit cell (r_e)	1.13 m (spacing: 2 m); 1.695 m (spacing: 3 m)	0.565 m
	Stress concentration ratio (n_s)	7	1
	Radius factor of clogging (α)	As given in Fig. 12	1
	Permeability factor for clogging (α_k)		1

[a]Assumed for the present analysis after Han and Ye (2002).
[b]Assumed for the present analysis after Walker and Indraratna (2006).
[c]Assumed for the present analysis.

excess pore pressure was normalized by the applied vertical stress on the ground surface. Excess pore pressure asymptotically decreases with time. The resistance to excess pore pressure dissipation caused by clogging is observed as well.

The normalized ground settlement with and without clogging is presented in Fig. 7(c). The average ground settlement asymptotically increases with time. The effect of clogging is found to influence the pattern of settlement at an initial stage of consolidation ($0 < T_r < 0.04$) as α increases from 0.5 to 1.0. However, because the stress distribution remains unaltered, the ultimate values of settlement seem to be the same, and the effect of clogging only retards the rate of consolidation.

The vertical stress distributions on the ground surface for the values of n_s as 5, 10, and 15 are presented in Fig. 8(a), whereas the typical settlement profiles in the unit cell at time 100, 250, and 400 days with and without clogging are shown in Figs. 8(b and c), respectively. All the ground settlement profiles are observed to be parabolic in shape, with the slope gradually diminishing with radial distance to zero at the unit cell boundary. When clogging is ignored, the ground settlement at the interface remains steady. The clogging effect initiates progressive increase of the ground settlement at the interface with time. This is understandable because the excess pore water pressure always remains zero at the interface for $t > 0$ as per the boundary condition adopted for the unclogged stone column, whereas the excess pore pressure gradually diminishes with time when clogging is considered.

The stone columns with higher strength and stiffness carry a greater vertical stress on the top with respect to the surrounding soil. The pattern of variation between the stresses on the stone column and the soil and the corresponding stress concentration ratio n_s was studied. Figs. 9(a and b) show the plots between the average vertical stresses on the top of the column (q_c) and the soil surface of the unit cell (q_{av}), respectively, normalized by the overall vertical stress ($=q_s + \gamma_e H_e$) and the stress concentration ratio n_s. With an increase in the normalized vertical stress on the column within the range 2.3–6.3, the resulting stress concentration ratio n_s has been observed to increase sharply from 2 to 14 following a hyperbolic pattern with increasing slope [Fig. 9(a)]. The rate of stress increment is significantly high in the range of $2 < n_s < 8$ and stabilizes thereafter. On the contrary, with the increase in the average stress on the soil surface from 0.1 to 0.5, the parameter n_s is observed to decreases almost exponentially [Fig. 9(b)].

Apart from the strength and stiffness of the soft clay and the stone column material, the radius and spacing of the stone columns are the important design parameters for a reinforced soil-stone column system. With this in mind, the effect of the parameter N and H/r_c on the settlement and consolidation parameters is examined. The ranges of values of these two parameters were chosen as 2–5, and 25–40, respectively, which are close to the field values. Within the selected range of N and H/r_c in the present analysis, the settlement factor ξ is observed to vary from 0.70 to 0.92 [Fig. 10(a)]. With an increase in N, the value of ξ is observed to increase in a curvilinear manner, with a stable trend for $N > 3.5$. Conversely, ξ decreases with H/r_c, as shown Fig. 10(b), but the rate of such decrease is marginal when $H/r_c \geq 30$.

In the semiempirical method suggested by Priebe (1995), the linear elastic theory was adopted to predict the settlement of the columnar-reinforced soft soil. Ellouze et al. (2010) pointed out several inconsistencies of the assumptions made in the method. The present model computes the settlement of the soft ground and considers the volumetric compressibilities of the soil and that of the column using the radial consolidation theory. Conversely, the settlement of the unreinforced soft soil is calculated from Terzaghi's one-dimensional consolidation theory. Hence, the computed settlements are essentially time dependent. Kempfert (2003) and Raithel et al. (2005) suggested that the settlement factor ξ varies in the range of 0.4–20. However, because of a different column to soil stiffness ratio, the average settlement of the reinforced soil at a specified degree of consolidation should be lower compared with that of the untreated soft ground, which essentially implies that $\xi < 1$. In the current analysis, the computed range of 0.70–0.92 of the settlement factor ξ is in agreement with the available literature and is therefore logical.

The variation of the time required for a specified degree of consolidation with N is studied [Fig. 10(c)]. A modified time factor

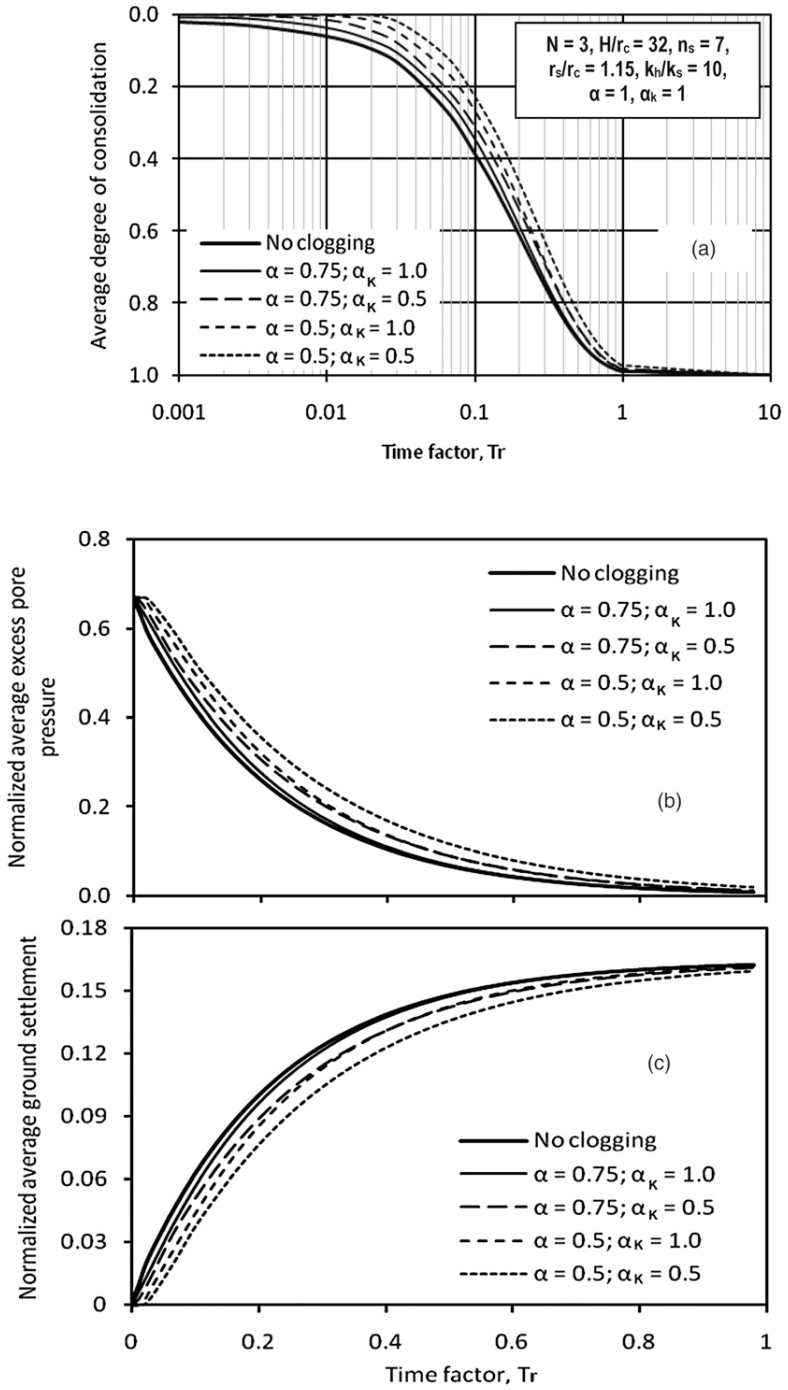

Fig. 7. Time variation of (a) average degree of consolidation; (b) average excess pore pressure; (c) normalized average ground settlement

$T_r'(=c_{vr}t/H^2)$, which eliminates the effect of variation of r_c, was used to normalize the time. For achieving an average degree of consolidation of 90%, the normalized time increases with N following a curvilinear pattern, with the slope of the curves initially decreasing with increasing values of N in the range $2 < N < 3$ and thereafter slowly increasing for $N > 3$.

The variation of the improvement factor ω [see Eq. (20)] with time and imposed load intensity are examined in Fig. 11. On the basis of the stability analysis of the embankment, the imposed load needs to be less than 200 kPa to prevent failure. It is observed in Fig. 11(a) that ω increases sharply with time for $t < 10$ months ($T_r < 0.23$), after which the value of ω stabilizes asymptotically. With the increase in load intensity, ω increases fairly linearly as shown in Fig. 11(b). It is well known that the undrained shear strength of the surrounding soil depends on the amount of surcharge pressure and corresponding consolidation. At higher loading intensity, the surrounding soil will be subjected to a greater consolidation and hence attain higher undrained shear strength. In other words, at higher loads than the present loading conditions, a higher improvement factor will be attained. For the selected range of imposed load intensity on the ground surface, the improvement factor was observed to vary in the range of 2.94–8.5.

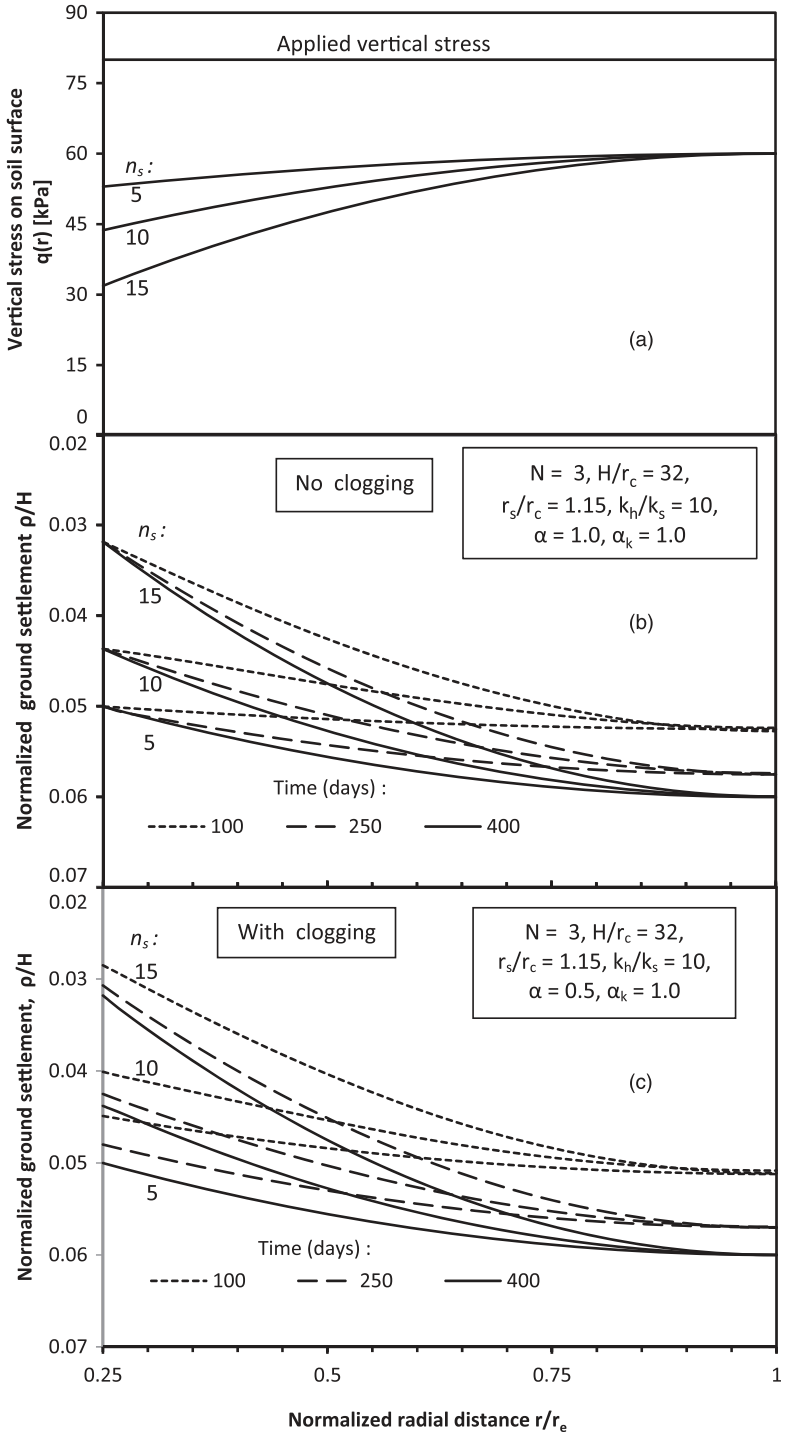

Fig. 8. Settlement analysis in the unit cell: (a) vertical stress distribution on the ground surface; (b) ground settlement profile considering no clogging; (c) ground settlement profile considering clogging

Special Case: Application of the Model to Prefabricated Vertical Drains

Apart from stone columns, the installation of prefabricated vertical drains (PVD) is one of the most popular techniques used worldwide for the improvement of soft clay (Indraratna 2009). In the case of PVDs, the distribution of the vertical stress on the ground surface is uniform (=the applied load intensity) as shown in Fig. 3(a), due to both the absence of stress concentration and insignificant arching. Also, clogging of PVDs is usually rare. Therefore, the proposed model can be applied to PVDs by ignoring the arching and clogging, taking $n_s = 1$, and modifying the stress distribution function as given by Eq. (8*d*) in the following form:

$$q(r) = q_s + \gamma_e H_e \tag{22}$$

J. Geotech. Geoenviron. Eng. 2013.139:377-394.

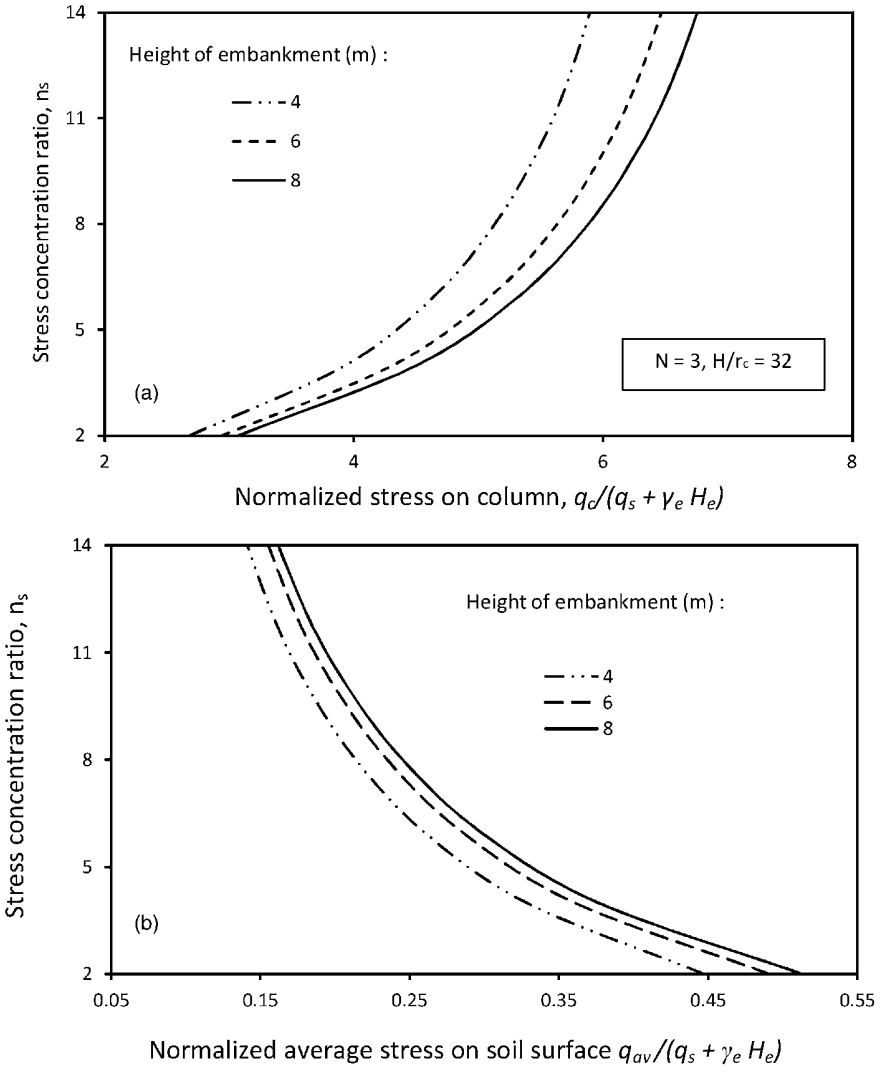

Fig. 9. Plot of n_s versus the average vertical stress on (a) column and (b) soil surface

Comparison of the present solution is made, as shown in Fig. 12(a), with the analytical solutions of Barron (1948) and Hansbo (1981) using the same computational parameters ($N = 2$, $k_h/k_s = 10$, $r_s/r_c = 1.1$, $H/r_c = 20$) except for $n_s = 1$. It is observed that the results obtained using the present model are quite close to those of Barron (1948) and Hansbo (1981).

A comparative analysis with the field test results of the Ballina Bypass (Indraratna 2009) was carried out. The Pacific Highway linking Sydney and Brisbane was constructed to reduce the high traffic congestion in Ballina. This bypass route must cross a floodplain consisting of highly compressible and saturated marine clay deposits. A system of surcharge load with PVDs was adopted to improve the geotechnical properties of the clay layers (Indraratna 2009). A soft silty layer of clay approximately 10 m thick was underlain by a moderately stiff, silty layer of clay located 10–30 m deep, which was in turn underlain by firm clay. The groundwater level almost coincided with the ground surface. The computational parameters used are in accordance with Indraratna (2009) and are given in Table 1. The construction stages of the embankment are shown in Fig. 12 (c). A coupled analysis was adopted, where the dissipation of excess pore pressure was assumed to occur during embankment construction. Each of the two ramp loadings was divided into 10 equal step loadings [Fig. 12(c)], and consolidation was allowed at each step. The time-settlement curve is shown in Fig. 12(b). It is observed that in the case of PVDs, the computed time-settlement curve is in good agreement with the field data, with an average deviation of only about 5%. For $t < 100$ days ($T_r < 0.23$), the computed settlement slightly underpredicts the field measurements. For $t > 100$ days, the field data plot below the predicted settlement.

Model Limitations

Although the proposed finite-difference model can predict the time-dependent response of stone column–reinforced soil to an acceptable accuracy, it has the following inherent limitations:

1. Although radial consolidation of soft ground with stone columns or PVDs is always accompanied by vertical flow (Han and Ye 2000), the latter was ignored in the present analysis.

J. Geotech. Geoenviron. Eng. 2013.139:377-394.

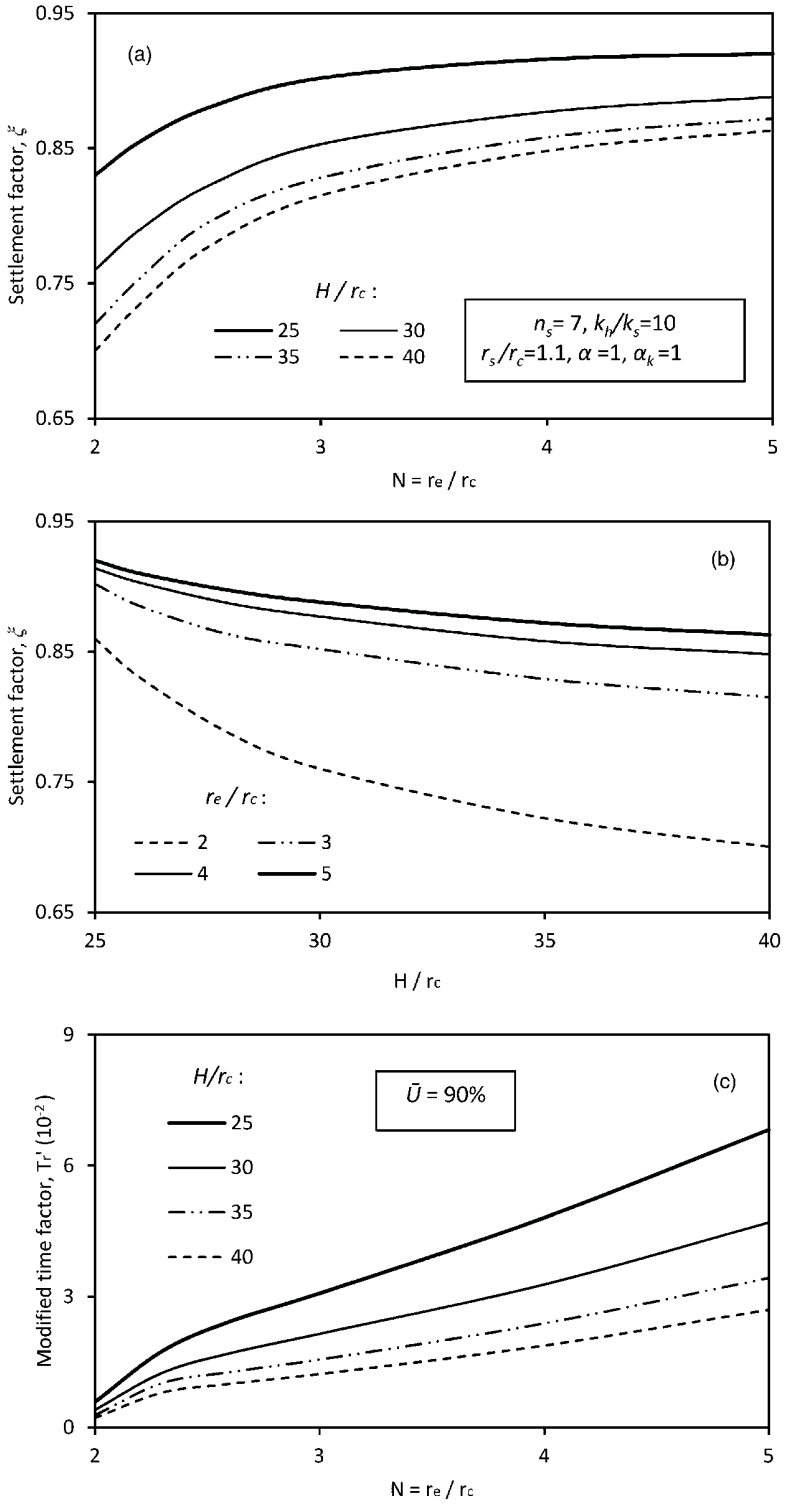

Fig. 10. Variation of (a) ξ with N; (b) ξ with H/r_c; and (c) T_r' with N

The role of vertical flow becomes more significant when the columns become shorter.

2. When a soft clay deposit overlies a sand bed, Assumption 4 in section Assumptions is no longer valid. The model should not be used under these circumstances.
3. When considering the clogging effect, the value of the parameter α was assumed to remain constant throughout the process of consolidation, whereas in reality, α may decrease progressively from unity for freshly installed columns to a lower value with time.
4. Although the model can analyze the consolidation of soft clay under conventional step loading (i.e., at a rest period), it is unable to accommodate the time-dependent ramp or cyclic loadings.

J. Geotech. Geoenviron. Eng. 2013.139:377-394.

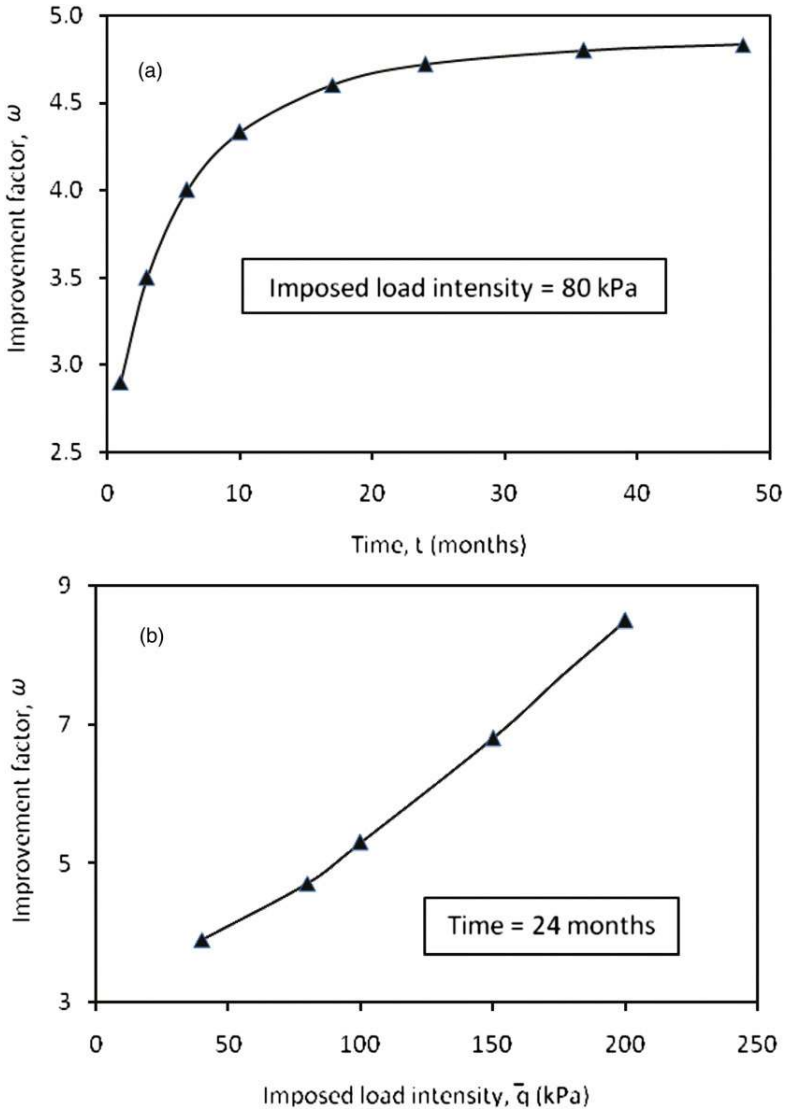

Fig. 11. Variation of improvement factor ω with (a) time and (b) imposed load intensity

Conclusions

A finite-difference solution for predicting the stress distribution and consolidation response of stone column–reinforced soft ground based on the unit cell concept was developed based on the free strain hypothesis, considering arching, smear, and clogging effects. The comparison of the numerical results with the available field data and past theoretical studies justifies the validity of the proposed model.

The study indicates that the clogging in the stone column retards the overall consolidation process. The average ground settlement increases with time, the rate of which stabilizes in an asymptotic manner. The effect of clogging was found to influence the pattern of settlement at the initial stage of consolidation ($0 < T_r < 0.04$) as α increases from 0.5 to 1.0. Because the stress distribution remains unaltered, the ultimate values of settlement remain the same, and the effect of clogging only retards the rate of settlement consolidation. The typical settlement profile is observed to be parabolic, with the slope gradually diminishing with the radial distance to zero at the unit cell boundary. When clogging is ignored, the ground settlement at the interface does not vary with time. Conversely, incorporation of clogging leads to progressive increase of the ground settlement at the interface with time.

The vertical stress distribution acting on the column and the soil surface of the unit cell are significantly affected by the relative stiffness of the column and the soil. With an increase in the normalized vertical stress on the column within the range 2.3–6.3, the resulting stress concentration ratio is observed to increase sharply in the range of $2 \leq n_s \leq 14$ following a hyperbolic pattern with increasing slope. The rate of stress increment is significantly high in the range of $2 < n_s < 8$ and stabilizes thereafter. On the contrary, with the increase in the average stress on the soil surface from 0.1 to 0.5, the parameter n_s is observed to decrease almost exponentially.

The magnitude of ground settlement is influenced by the variation of the radius and spacing of stone columns. When the parameters N and H/r_c varied from 2 to 5 and 25 to 40, respectively, the settlement factor ξ varied from 0.70 to 0.92. The value of ξ increases with N and stabilizes asymptotically when $N > 3.5$. Conversely,

J. Geotech. Geoenviron. Eng. 2013.139:377-394.

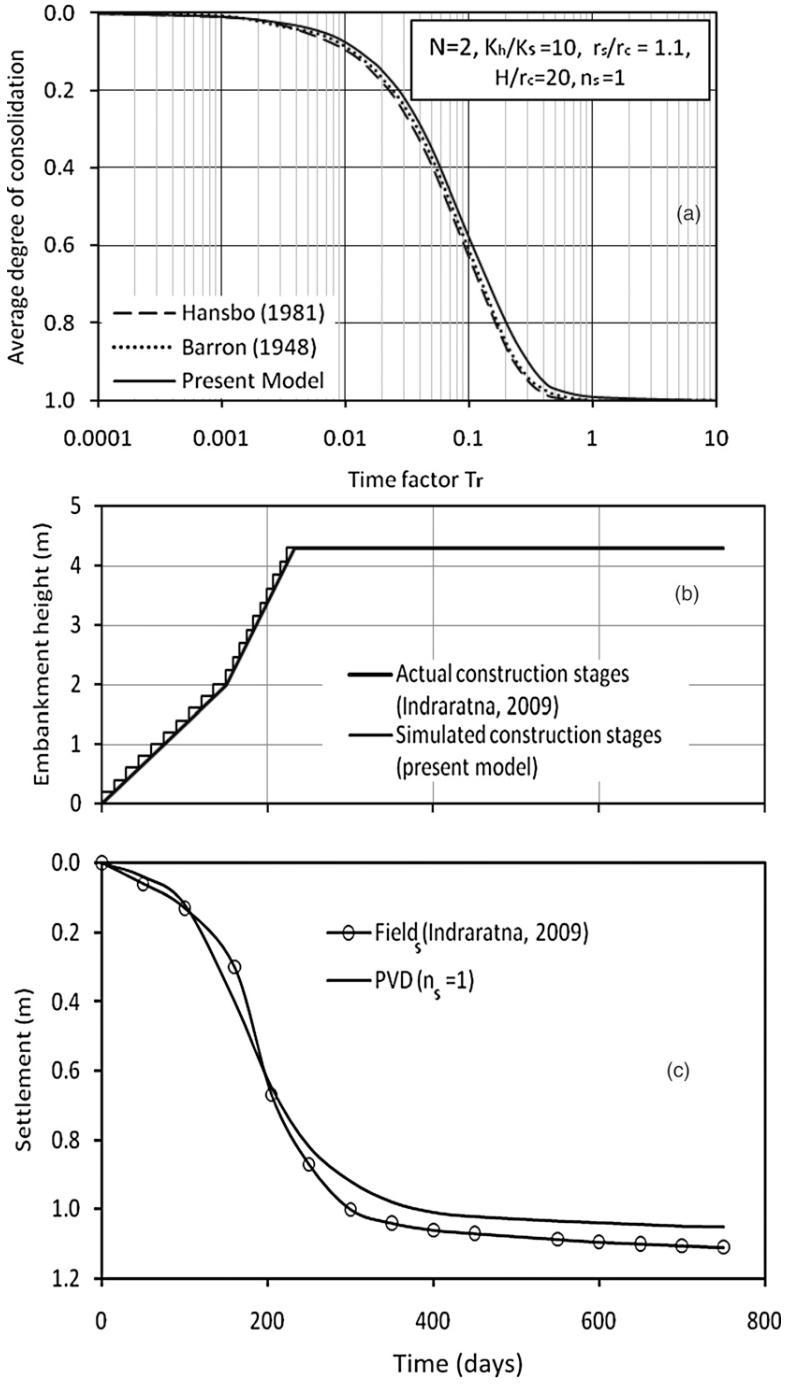

Fig. 12. Application of the proposed model with PVD: (a) comparison with existing models of Barron (1948) and Hansbo (1981); (b) actual and simulated construction stages; (c) comparison of average ground surface settlement with field data of Indraratna (2009)

ξ decreases with H/r_c, but the rate of this decrease is marginal when $H/r_c \geq 30$. The time required to achieve a specified average degree of consolidation increases in a curvilinear manner with N. For 90% consolidation, the slope of the curves is observed to decrease with increasing N in the range $2 < N < 3$ and thereafter increases slowly.

The improvement factor ω introduced in this study represents the ratio of the minimum value of the instantaneous to initial undrained shear strength of the soil at ground level. When $T_r < 0.23$, the value of ω increases quite sharply with time but stabilizes asymptotically thereafter. With an increase in the load intensity, the value of ω increases fairly linearly.

The proposed model could also be used to predict the performance of ground improved with PVDs by ignoring the arching and the clogging and taking $n_s = 1$. The results obtained using the present model were quite close to those of Barron (1948) and Hansbo (1981). A comparative study carried out with the field test results of the Ballina Bypass (Indraratna 2009) indicated good agreement, with an average deviation of within about 5%.

J. Geotech. Geoenviron. Eng. 2013.139:377-394.

Appendix. Mathematical Derivations

Considering the ring element shown in Fig. 4, the volume of water out of the soil mass through the inner vertical surface at time interval dt is given as

$$V_o = (k_h/\gamma_w)\frac{\partial u}{\partial r}2\pi r\,dz\,dt \tag{23}$$

where γ_w = unit weight of water.
Similarly, the flow of water into the soil mass through the outer vertical surface is given by

$$V_i = (k_h/\gamma_w)\frac{\partial}{\partial r}\left(u + \frac{\partial u}{\partial r}dr\right)2\pi(r + dr)\,dz\,dt \tag{24}$$

Therefore, the net reduction in the volume of the soil element at time interval dt is given (neglecting the higher order term) by

$$\begin{aligned} dV &= V_o - V_i = (k_h/\gamma_w)\left(\frac{1}{r}\frac{\partial u}{\partial r} + \frac{\partial^2 u}{\partial r^2}\right)2\pi r\,dr\,dz\,dt \\ &= -(k_h/\gamma_w)\left(\frac{1}{r}\frac{\partial u}{\partial r} + \frac{\partial^2 u}{\partial r^2}\right)V dt \end{aligned} \tag{25}$$

where V = volume of the soil mass at time $t = 2\pi r\,dr\,dz$.
The matrices in Eq. (11) are described:

$$\{u\} = \{u_{11}, u_{12}, u_{13}, \ldots,\ u_{1p},\ u_{21}, u_{22}, u_{23}, \ldots,\ u_{2p},\ u_{31}, u_{32}, u_{33}, \ldots,\ u_{3p}, \ldots\ldots,\ u_{m1}, u_{m2}, u_{m3}, \ldots, u_{mp}\}^T$$

$$\{b\} = \{u_0(1),0,0,\ldots,0,\ u_0(2),0,0,\ldots,0,\ u_0(3),0,0,\ldots,0,\ldots\ldots\ldots,\ u_0(m),0,0,\ldots,0\}^T$$

$$[A] = \begin{bmatrix} a_{11} & a_{12} & a_{13} & \ldots\ldots & a_{1,mp} \\ a_{21} & a_{22} & a_{23} & \ldots\ldots & a_{2,mp} \\ a_{31} & a_{32} & a_{33} & \ldots\ldots & a_{3,mp} \\ - & - & - & - & - \\ - & - & - & - & - \\ a_{mp,1} & a_{mp,2} & a_{mp,3} & \ldots\ldots & a_{mp,mp} \end{bmatrix} \ldots\ldots \tag{26}$$

The coefficients a_{ij} of the matrix $[A]$ are obtained from Eq. (10) and by applying the boundary conditions given in section Consolidation of Soft Clay.
The compression of the soil element (Fig. 4) in the time interval dt is given [using Eq. (10)] by

$$d\rho = \frac{dV}{2\pi r dr} = (k_h/\gamma_w)\left(\frac{1}{r}\frac{\partial u}{\partial r} + \frac{\partial^2 u}{\partial r^2}\right)dz\,dt = -m_v\frac{\partial u}{\partial t}\,dz\,dt \tag{27}$$

The preceding expression can be integrated to compute the displacement of a point (r, z) within the soil mass of the unit cell at time instant t, and accordingly, Eq. (14) is obtained.
From the e-σ' relationship of the soft clay

$$\frac{e_0 - e(i,j,k)}{\sigma'(i,j,k) - \sigma'_0} = m_{vi}(1 + e_0) \tag{28}$$

where σ'_0 is the initial effective stress in the soil at the nodal point under consideration. Eq. (28) can be rewritten as

$$\frac{\sigma'(i,j,k)}{\sigma'_0} = \frac{1}{1 - \dfrac{e_0 - e(i,j,k)}{m_{vi}(1 + e_0)\sigma'(i,j,k)}} \tag{29}$$

Following the analysis of Umezaki et al. (1993) regarding the constant value of the undrained shear strength ratio of the soil irrespective of the consolidation time, Eq. (19) was derived using Eq. (29).

Acknowledgments

The authors gratefully acknowledge the financial support received in the form of an Endeavour Postdoctoral Research Fellowship from the Department of Education, Environment and Workplace Relations (DEEWR), Australian Government, through Austraining International.

Notation

The following symbols are used in this paper:

$[A]$ = coefficient matrix;
a_{ij} = elements of the finite difference coefficient matrix;
$\{b\}$ = augment vector;
c_u = undrained cohesion;
c_{u0} = initial undrained cohesion at ground level;
c_{vr} = coefficient of radial consolidation of the soil;
E_c, E_s = elastic moduli of the column and the surrounding soil;
e = void ratio;
e_0 = initial void ratio;
H = thickness of the soft clay deposit;
H_e = height of embankment;
i = radial coordinate indicator;
j = depth coordinate indicator;
K_p = passive earth pressure coefficient of the embankment;
k = time coordinate indicator;
k_{cl} = horizontal permeability of clogged zone;
k_h = horizontal soil permeability;
k_s = horizontal permeability of smear zone;
k_0 = in situ earth pressure coefficient at rest;
m_v = soil volume compressibility;
m_{vc} = volumetric compressibility of the column;
m_{vi} = soil volume compressibility at the ith node;

J. Geotech. Geoenviron. Eng. 2013.139:377-394.

m, n, p = number of divisions;
N = r_e/r_c;
n_s = ratio of the volumetric compressibility of the soil to that of the column;
q = average vertical stress on unit cell upper boundary;
q_{av} = average vertical stress on the soil surface of the unit cell;
q_c = average vertical stress on top of column;
q_s = surcharge load intensity on embankment surface;
q_1 = vertical stress on ground surface on soil at interface;
q_2 = vertical stress on ground surface on soil at unit cell boundary;
$q(r)$ = vertical stress on ground surface at radial distance r;
R = global radial coordinate;
r = radial coordinate of unit cell;
r_c = radius of stone column;
r_c' = radius of stone column excluding the clogged zone;
r_e = radius of influence of one stone column;
r_s = radius of smear zone;
T_r = time factor = $c_{vr}t/(4r_{e^2})$;
T_r' = modified time factor = $c_{vr}t/H^2$;
t = time coordinate;
t_t = total time of consolidation;
U = degree of consolidation;
U_t = average degree of consolidation;
u = excess pore water pressure;
$\{u\}$ = excess pore water pressure vector;
u_t = average excess pore water pressure at any time t;
V = volume of soil mass;
z = depth coordinate;
α = radius factor for clogging;
α_k = permeability factor for clogging;
γ' = effective unit weight of soil;
γ_e = unit weight of fill;
γ_w = unit weight of water;
δ_t = length of an element on time axis;
δ_r = length of an element on radial axis;
δ_z = length of an element on depth axis;
ε = vertical compressive strain in soil;
ε_v = volumetric strain in soil;
ζ_c = rate of increase in undrained cohesion of soil;
θ = global coordinate;
ξ = settlement factor;
ρ = vertical displacement of soil;
$\overline{\rho}_{u90}$ = average settlement at ground surface of the unreinforced soil at 90% consolidation;
$\overline{\rho}_{90}$ = average settlement at ground surface of the reinforced soil at 90% consolidation;
σ' = effective stress in soil;
σ_R = normal stress in soil element along R-direction;
σ_θ = normal stress in soil element along θ-direction;
χ = a Poisson's ratio function for the soil and the column; and
ω = improvement factor.

References

Abusharar, S. W., Zheng, J. J., Chen, B. B., and Yin, J. H. (2009). "A simplified method for analysis of a piled embankment reinforced with geosynthetics." *Geotextiles Geomembranes*, 27(1), 39–52.

Adalier, K., and Elgamal, A. (2004). "Mitigation of liquefaction and associated ground deformations by stone columns." *Eng. Geol.*, 72(3–4), 275–291.

Alamgir, M., Miura, N., Poorooshasb, H. B., and Madhav, M. R. (1996). "Deformational analysis of soft ground reinforced by columnar inclusions." *Comput. Geotech.*, 18(4), 267–290.

Balaam, N. P., Poulos, H. G., and Brown, P. T. (1977). "Settlement analysis of soft clays reinforced with granular piles." *Proc., 5th Southeast Asian Conf. on Soil Engineering*, Sponsor Southeast Asian Geotechnical Society, Bangkok, Thailand, 81–92.

Barksdale, R. D., and Bachus, R. C. (1983). "Design and construction of stone columns." *Rep. FHWA/RD-83/026*, National Technical Information Service, Springfield, VA.

Barron, B. A. (1948). "Consolidation of fine grained soil by drain wells." *Trans. Am. Soc. Civ. Eng.*, 113(2346), 712–748.

Castro, J., and Sagaseta, C. (2009). "Consolidation around stone columns: Influence of column deformation." *Int. J. Numer. Anal. Methods Geomech.*, 33(7), 851–877.

Deb, K. (2010). "A mathematical model to study the soil arching effect in stone column-supported embankment resting on soft foundation soil." *Appl. Math. Model.*, 34(12), 3871–3883.

Ellouze, S., Bouassida, M., Hazzar, L., and Mroueh, H. (2010). "On settlement of stone column foundation by Priebe's method." *Ground Improv.*, 163(GI2), 101–107.

Guetif, T., Bouassida, M., and Debats, J. M. (2007). "Improved soft clay characteristics due to stone column installation." *Comput. Geotech.*, 34(2), 104–111.

Hajra, M. G., Reddi, L. N., Glasgow, L. A., Xiao, M., and Lee, I. M. (2002). "Effects of ionic strength on fine particle clogging of soil filters." *J. Geotech. Geoenviron. Eng.*, 128(8), 631–639.

Han, J., and Ye, S. L. (2000). "Simplified method for consolidation rate of stone column reinforced foundations." *J. Geotech. Geoenviron. Eng.*, 127(7), 597–603.

Han, J., and Ye, S. L. (2002). "A theoretical solution for consolidation rates for stone column reinforced foundations accounting for smear and well resistance effects." *Int. J. Geomech.*, 2(2), 135–151.

Hansbo, S. (1981). "Consolidation by vertical drains." *Geotechnique*, 31(1), 45–66.

Indraratna, B. (2009). "Recent advances in the application of vertical drains and vacuum preloading in soft clay stabilization." *Austral. Geomechan. J.*, 45(2), 1–44.

Indraratna, B., Balasubramaniam, A., and Balachandran, S. (1992). "Performance of test embankment constructed to failure on soft clay." *J. Geotech. Eng.*, 118(1), 12–33.

Indraratna, B., and Redana, I. W. (1997). "Plane strain modelling of smear effects associated with vertical drains." *J. Geotech. Eng.*, 123(5), 474–478.

Indraratna, B., and Redana, I. W. (1998). "Laboratory determination of smear zone due to vertical drain installation." *J. Geotech. Eng.*, 125(1), 96–99.

Kempfert, H. G. (2003). "Ground improvement methods with special emphasis on column-type techniques." *Int. Workshop on Geotechnics of Soft Soils–Theory and Practice*, Taylor & Francis Group, New York, 101–112.

Khan, A. P., Madhav, M. R., and Reddy, E. S. (2010). "Consolidation of thick clay layer by radial flow—Nonlinear theory." *Geotech. Eng.*, 2(2), 157–160.

Lo, S. R., Zhang, R., and Mak, J. (2010). "Geosynthetic-encased stone columns in soft clay: A numerical study." *Geotextiles Geomembranes*, 28(3), 292–302.

Lorenzo, G. A., and Bergado, D. T. (2003). "New consolidation equation for soil-cement pile improved ground." *Can. Geotech. J.*, 40(2), 265–275.

Low, B. K., Tang, S. K., and Choa, V. (1994). "Arching in piled embankments." *J. Geotech. Eng.*, 120(11), 1917–1938.

Malarvizhi, S. N., and Ilamparuthi, K. (2008). "Numerical analysis of encapsulated stone columns." *Proc., 12th Int. Conf. of IACMAG*, Centre for Infrastructure Engineering and Safety, Sydney, Australia, 3719–3726.

Mays, D. C. (2010). "Contrasting clogging in granular media filters, soils, and dead-end membranes." *J. Environ. Eng.,* 136(5), 475–480.
Mitchell, J. K. (1981). "Soil improvement—State of the art report." *Proc., 10th ICSMFE*, Vol. 4, Balkema, Rotterdam, Netherlands, 509–565.
Murugesan, S., and Rajagopal, K. (2010). "Studies on the behavior of single and group of geosynthetic encased stone columns." *J. Geotech. Geoenviron. Eng.,* 36(1), 129–139.
Oh, E. Y. N., et al. (2007). "Behaviour of a highway embankment on stone column improved estuarine clay." *Proc., 16th Southeast Asian Geotechnical Conf.*, Vol. 1, Southeast Asian Geotechnical Society, Bangkok, Thailand, 567–572.
Priebe, H. J. (1995). "The design of vibro replacement." *Ground Eng.*, 28(10), 31–37.
Raithel, M., Kirchner, A., Schade, C., and Leusink, E. (2005). "Foundation of constructions on very soft soils with geotextile encased columns: State of the art," *Geo-Frontiers 2005*, Vol. 130–142, ASCE, Reston, VA, 1867–1877.
Reddi, L. N., Ming, X., Hajra, M. G., and Lee, I. M. (2000). "Permeability reduction of soil filters due to physical clogging." *J. Geotech. Geoenviron. Eng.,* 126(3), 236–246.
Terzaghi, K. (1943). *Theoretical soil mechanics*, Wiley, New York.
Umezaki, T., Ochiai, H., and Hayashi, S. (1993). "Undrained shear strength of clay during consolidation." *Proc., 11th Southeast Asian Geotechnical Conf.*, Southeast Asian Geotechnical Society, Bangkok, Thailand, 269–274.
Walker, R., and Indraratna, B. (2006). "Vertical drain consolidation with parabolic distribution of permeability in smear zone." *J. Geotech. Geoenviron. Eng.,* 132(7), 937–941.
Wang, G. (2009). "Consolidation of soft soil foundations reinforced by stone columns under time dependent loading." *J. Geotech. Geoenviron. Eng.,* 135(12), 1922–1931.

J. Geotech. Geoenviron. Eng. 2013.139:377-394.